Fluctuation and Noise Letters
Vol. 0, No. 0 (2001) 000–000
© World Scientific Publishing Company

# OPTIMAL DIFFUSIVE TRANSPORT IN A TILTED PERIODIC POTENTIAL

Benjamin Lindner, Marcin Kostur, and Lutz Schimansky-Geier
*Institute of Physics, Humboldt-University Berlin*
*Invalidenstr.110 D-10115 Berlin, Germany*

Received (24 January 2001)
Revised (8 February)
Accepted (12 February)

We study the diffusive motion of an overdamped Brownian particle in a tilted periodic potential. Mapping the continuous dynamics onto a discrete cumulative process we find exact expressions for the diffusion coefficient and the Péclet number which characterize the transport. At a sufficiently strong but subcritical bias an optimized transport with respect to the noise strength is observed. These results are confirmed by numerical solution of the Fokker-Planck equation.

*Keywords*: Brownian motion; diffusion; periodic potentials; transport.

## 1. Introduction

There are many examples of stochastic dynamics which can be described by the Brownian motion in a tilted washboard potential ranging from mathematical pendulum with dissipation and noise [1] over superionic conduction [2] to neuronal activity [3, 4]. The qualitative asymptotic behavior of the system is well known. Expressed in terms of real Brownian motion, particles in a tilted washboard subjected to friction and noise will diffuse and drift in the direction of the bias. The determination of mean velocity and effective diffusion coefficient, however, was a challenging task for decades and can be performed in the general damped case only by simulations or by a numerical solution of the Fokker-Planck equation [1].
The *overdamped* limit of this model in turn can be treated analytically to a great extent. Already in 1958, Stratonovich [5] derived a closed expression for the stationary mean velocity and gave also an approximate expression for the effective diffusion coefficient. During the 1970's, an exact expression for the diffusion coefficient could be calculated for the special case of vanishing bias [6]. Another approximation for a *finite* bias has been proposed recently [7].
Stratonovich's approach to the diffusion coefficient holds true for a weak tilting of the potential and small noise intensity. In this case the particle rarely jumps

from one potential minimum into the next one to the right or left, respectively, whereby one of the directions is preferred due to the bias. Stratonovich assumed in this regime that the process can be modeled by a biased random walk. Thus, the diffusion coefficient is determined by the rate from the minimum to the left and right potential barriers (maxima of the potential). This approach neglects the relaxation time from barrier to minimum that becomes relevant for stronger tilt. It fails completely for a so called supercritical tilt for which minima and maxima of the potential vanish since in this case the process cannot be described by a Poissonian hopping process anymore. In the case of a very strong tilt, however, the situation is simplified again since the potential shape can be ignored and the diffusion coefficient coincides with that of free diffusion.

The transport of particles is characterized by an average motion in direction of the bias and the counteracting spreading effect due to the presence of noise. While the drift may be desired the dispersion is an unwanted but - especially in case of a subcritical bias - inevitable side effect. Coherent transport refers to the case of large mean velocity at fairly small diffusion. It can be best quantified by the nondimensional Péclet number, i.e., a proper ratio of mean velocity to effective diffusion coefficient. Clearly, the transport is most coherent when this number is maximal.

In this paper we address a situation where the minima and maxima of the effective potential are still present (subcritical tilt) but the tilt is sufficiently strong that the relaxation time scale has to be taken into account. We will restrict ourselves to the overdamped case and derive exact expressions for the diffusion coefficient and the Péclet number. It will be shown that a large relaxation time scale can lead to a coherent (regular) transport of particles when the noise strength is optimally chosen. This is manifested by a maximum of the Péclet number with respect to the noise intensity. We will illustrate the meaning of this maximum in terms of the time dependent probability density of particles.

Furthermore, for specific potential shapes another quality of coherence appears. If a flat potential with small sharp maxima is sufficiently tilted the effective diffusion coefficient itself attains a local minimum as a function of the noise intensity. The surprising effect that increasing noise decreases diffusion is explained by the occurrence of a large ratio of relaxation to escape time for a certain range of noise intensities.

Regarding the calculation of the diffusion coefficient for finite bias, independent work by Reimann et. al. [8] has been done although the approach as well as the physical phenomenon considered in that study differ much from ours.

The paper is organized as follows. In section 2 we introduce the model and the quantities of interest. In section 3 we outline the mapping onto a discrete cumulative process that permits the determination of asymptotic mean and variance of the original process. In sections 4 and 5 we turn to specific potential shapes and the phenomenon of coherent transport. Finally in section 6, we give a summary and discuss the close connection of our findings to *coherence resonance* encountered in excitable systems.

## 2. Model and quantities of interest

Consider the overdamped motion of a Brownian particle in a potential $U(x)$ with period $L$ subject to a tilting force $F$ and a white Gaussian noise

$$\dot{x} = -\frac{d}{dx}(U(x) - Fx) + \sqrt{2D}\xi(t). \tag{1}$$

Here, the friction coefficient $\gamma$ has been omitted realized by rescaling the force term and noise intensity $D$. The force in (1) is often written as the derivative of the *effective* potential $V(x) = U(x) - Fx$. If $U(x)$ is periodic there exists obviously a critical tilt $F_c$ where the corresponding minima and maxima vanish for $V(x)$.
The corresponding probability density for eq. (1) obeys the Fokker-Planck equation

$$\partial_t P(x,t) = \partial_x \left(V'(x) + D\partial_x\right) P(x,t). \tag{2}$$

An ensemble represented by $P(x,t)$ started at the sharp value $x_0 = 0$ moves in direction of the bias and spreads at the same time over several periods of the potential (cf. Fig. 1). For large times, the drift is characterized by the mean stationary velocity

$$v = \langle \dot{x} \rangle = \lim_{t\to\infty} \frac{\langle x(t) - x(0) \rangle}{t} \tag{3}$$

while the dispersion is quantified by the effective diffusion coefficient

$$D_{eff} = \frac{1}{2} \lim_{t\to\infty} \frac{\langle \Delta x(t)^2 \rangle}{t} = \frac{1}{2} \lim_{t\to\infty} \frac{\langle [x(t) - \langle x(t) \rangle]^2 \rangle}{t}. \tag{4}$$

The density itself tends asymptotically to

$$P_{as}(x,t) = P_0(x) \frac{\exp[-(x-vt)^2/4D_{eff}t]}{\sqrt{4\pi D_{eff} t}} \tag{5}$$

where $P_0$ refers to the stationary (necessarily periodic) solution of eq. (2) [1] with the special normalization $\int_0^L dx P_0(x) = L$. Clearly, this function is responsible for the local structure (local minima and maxima) whereas the Gaussian part represents the coarse grained density (thick line in Fig. 1). The asymptotic mean and variance of the true density $P_{as}(x,t)$ coincide with those of the Gaussian factor as we have tacitly assumed in eq. (5). The Gaussian function can be numerically extracted from $P(x,t)$ in different ways (cf. Fig. 1). One may fit $P(x,t)$ to a Gaussian function, filter the density (Fourier transformation, cutting off the high frequencies and perform the back transformation) or carry out a direct coarse graining by $\tilde{P}(\tilde{x},t) = \int_{\tilde{x}-L/2}^{\tilde{x}+L/2} dx P(x,t)/L$ with $\tilde{x} = x_0 + kL, k \in Z$. All three methods yield a satisfying agreement. For the data in Fig. 1 the fitted and filtered functions coincide within line thickness while the histogram obtained from the coarse graining seems to be the discrete counterpart to these functions.
It might be desired that particles started at a sharp value should reach a certain region without much spreading. An optimal transport in this sense is realized at large velocity and small diffusion and will result in a large Péclet number

$$Pe = \frac{vL}{D_{eff}}. \tag{6}$$

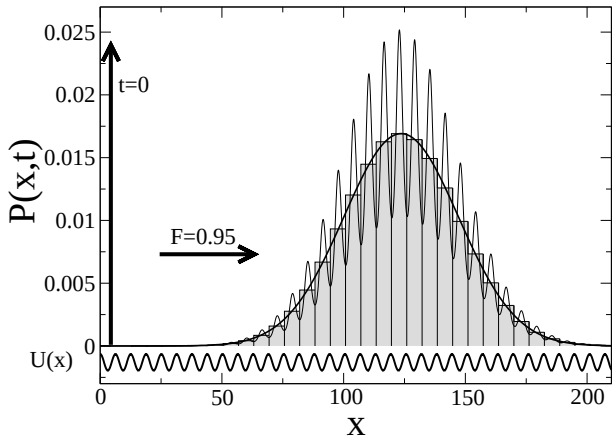


Fig 1. Evolution of the density $P(x,t)$ (thin line) for the potential $U(x) = \cos(x)$, $F = 0.95$ and $D = 2.05$. The density started at $x = 4.4$ (arrow) is calculated by a numerical solution of eq. (2). Additionally shown: the coarse grained density (histogram) and a fit of $P(x,t)$ to a Gaussian function (thick line) which coincides in line thickness with a filtered version of $P(x,t)$ (not shown). The potential $U(x)$ is drawn at the bottom for comparison.

This nondimensional ratio was frequently used in convection problems [9] and also recently applied to the transport problem in ratchet potentials [10].
Beside the trivial case of vanishing potential $U(x) \equiv 0$ (then $v = F$, $D_{eff} = D$), the usual approach to the diffusion problem posed by eq. (4) is to extract the diffusion coefficient from the time dependent solution of the Fokker-Planck equation (2). This works, e.g. in case of piecewise constant potential $U(x)$ [1], however, for a general periodic potential the time dependent solution is not available. Another way is to use a generalized fluctuation-dissipation relation [1]. However, this applies only in case of equilibrium systems, i.e., for vanishing tilt ($F = 0$) and results in an approximate formula for a system with finite bias [7].
Our approach utilizes the fact that the diffusion is entirely determined by the local properties of the system due to the periodicity of the potential. This allows a mapping onto a discrete process yielding the coarse grained density the asymptotic variance of which can be easily calculated.

## 3. Theory

The process described by eq. (1) is physically equivalent to the motion of a particle in an infinite ordered set of segments of the effective potential $V(x)$ as sketched in Fig. 2. The spatial overlap between subsequent segments is given by one period $L$ while the length of a single segment is $2L$. Whenever the particle reaches the left or right boundary it is absorbed and reinjected in the respective neighboring segment. These jump events have no physical meaning since coordinates and potential forces at absorption and injection points coincide. The probability in the $n$-th segment $P_n(x,t)$ obeys a FPE like (2) with absorbing boundary conditions and with an additional source of probability corresponding to the particle injection in the middle of the segment (see reference [11] for technical details of a similar system of FPE's).

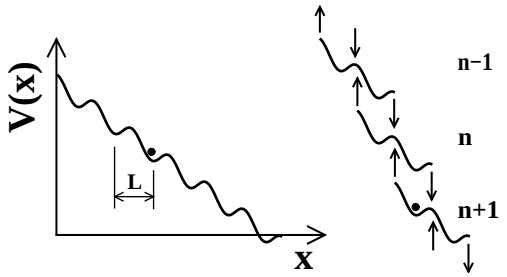


Fig 2. The motion of the particle (circle) in the tilted periodic potential $V(x)$ (left) is equivalent to that one in an infinite number of segments of the potential (right) with length $2L$. The arrows indicate transitions from one segment to the other.

The true density $P(x,t)$ from eq. (2) is given by the sum of these densities $P_n(x,t)$.

The seemingly complicated mapping onto the system of segments allows a rough discrete determination of the particle's position in terms of the segment $n_t$. Choosing the boundaries of the segments such that $x = 0$ (starting point) is in the middle of the segment with $n = 0$, we can approximate $x(t) \approx Ln_t$ with an uncertainty $\Delta x = \pm L$ at any time $t$. It is evident that in the asymptotic limit $t \to \infty$

$$\langle x(t)\rangle = L\langle n_t\rangle \ , \ \langle \Delta x(t)^2\rangle = L^2\langle \Delta n_t^2\rangle \tag{7}$$

holds true. The process $n_t$ illustrated in Fig. 3 (r.h.s.) emerges to be a cumulative process with independent increments (see appendix) for which asymptotic mean and variance can be easily found [12]. They are expressed by the first two central moments $\mu$ and $\sigma^2$ of the escape time density for a single segment depicted in Fig. 3 (l.h.s.). From these formulae and by virtue of eqs. (7), (3), (4), and (6) we find

$$v = L\frac{p_+ - p_-}{\mu} \tag{8}$$

$$D_{eff} = \frac{L^2}{2}\left(\frac{1}{\mu} + \frac{(p_+ - p_-)^2}{\mu^3}(\sigma^2 - \mu^2)\right) \tag{9}$$

$$Pe = 2\frac{p_+ - p_-}{1 - (1 - \frac{\sigma^2}{\mu^2})(p_+ - p_-)^2}. \tag{10}$$

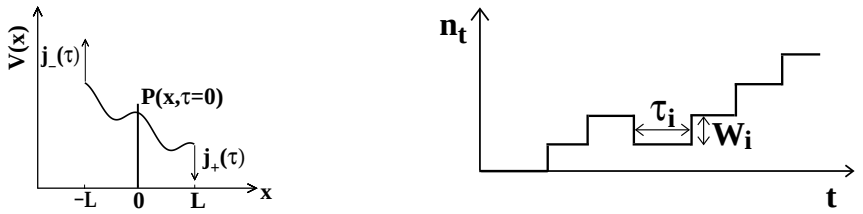


Fig 3. Left: The problem of escape from a single well. The initial condition $P(x, \tau = 0) = \delta(x)$ is indicated by a line. $j_-(\tau), j_+(\tau)$ denote out currents of probability. Right: a sample trajectory of the process $n_t$. The random increments $W_i \in \{-1, 1\}$ and the intervals $\tau_i$ correspond to independent realizations of the escape problem sketched at the l.h.s.

Therein, $p_-$ and $p_+$ denote the total probability to escape from the segment via the left and right boundary, respectively which are given by [13]

$$p_+ = 1 - p_- = \frac{1}{1 + e^{-\frac{FL}{D}}}. \tag{11}$$

The first two cumulants of the escape time density $\rho(\tau)$ can be calculated by standard formulae (see e.g. [13]). Assuming without loss of generality that the middle of the segment is at $x = 0$ and the boundaries are at $\pm L$ yields

$$\mu = \frac{1}{D(1 + e^{-\frac{FL}{D}})} \int_0^L dx e^{\frac{V(x)}{D}} \int_{x-L}^{x} dy e^{\frac{-V(y)}{D}} \tag{12}$$

$$\sigma^2 = \frac{2}{D(1 + e^{-\frac{FL}{D}})} \int_0^L dx e^{\frac{V(x)}{D}} \int_{x-L}^{x} dy e^{\frac{-V(y)}{D}} \left( T_1(y) - \frac{1}{2}\mu \right) \tag{13}$$

where $T_1(x)$ is given in terms of $\Phi(x) = \exp[V(x)/D]$ by

$$T_1(x) = \frac{\left( \int_{-L}^{x} dy\, \Phi(y) \right) \int_x^L dy \int_{-L}^{y} dz\, \frac{\Phi(y)}{\Phi(z)} - \left( \int_x^L dy\, \Phi(y) \right) \int_{-L}^{x} dy \int_{-L}^{y} dz\, \frac{\Phi(y)}{\Phi(z)}}{D \int_{-L}^{L} dy\, \Phi(y)}. \tag{14}$$

We stress that the relations (8),(9) and (10) are exact for an arbitrary shape of the periodic potential. The quadratures (12) and (13) have to be evaluated numerically, in general.
By inserting (12) into eq. (8) and an additional little manipulation of the integrals we recover the classic formula by Stratonovich (see, e.g. [1])

$$v = \frac{LD(1 - e^{-\frac{LF}{D}})}{\int_0^L dx\, e^{-\frac{V(x)}{D}} \int_x^{x+L} dy\, e^{\frac{V(y)}{D}}}. \tag{15}$$

For an *unbiased* potential ($F = 0$, i.e., $p_+ = p_-$) the velocity and Péclet number vanish trivially while the diffusion coefficient reduces to $L^2/2\mu$, i.e., to

$$D_{eff}(F = 0) = \frac{L^2 D}{\int_0^L dx e^{-U(x)/D} \int_0^L dy e^{U(y)/D}}. \tag{16}$$

Thus, we recover the well known result from [1].
On the other hand, according to Stratonovich's random walk assumption in case of a weak tilt, one may approximate $\sigma = \mu$ and again the second term in eq. (9) vanishes ($D_{eff} = L^2/2\mu$). In this case, the Péclet number approximatively reads

$$Pe(F \ll F_c) \approx 2(p_+ - p_-) = 2 \tanh(FL/2D). \tag{17}$$

the absolute value of which is a decreasing function of the noise intensity $D$.
We would like to point out a remarkable property for systems with symmetric potential $U(x) = U(-x)$. In this case, all calculated quantities do not change for the inverse potential $-U(x)$, for instance

$$U(x) = U(-x) \quad \Longrightarrow \quad D_{eff}[U(x)] = D_{eff}[-U(x)] \tag{18}$$

and likewise for $v$ and $Pe$. This can be proven by manipulations of the resulting quadrature formulae for $v$ and $D_{eff}$.
Finally, we remark that the above discretization by segments of length $2L$ is not the only valid choice. Reimann and coworkers [8] have implicitly used a mapping onto a set of infinitely long segments. They obtained the same result for the effective diffusion coefficient like in the present work (the proof is given in appendix Appendix B) and, furthermore, provided an elegant simplification of the quadratures.

## 4. Optimal transport in a cosine potential

Consider the archetypal potential $U(x) = \cos(x)$. The critical tilt at which the minima and maxima of the effective potential vanish is given by $F_c = 1$. For a strong but subcritical tilt $F = 0.95$, velocity and effective diffusion coefficient are increasing functions of the noise intensity (cf. Fig. 4, l.h.s.). The Péclet number, however, attains a maximum at a moderate value of $D$ indicating an optimal transport in this case. These findings are confirmed by results of a numerical solution of the FPE (2).

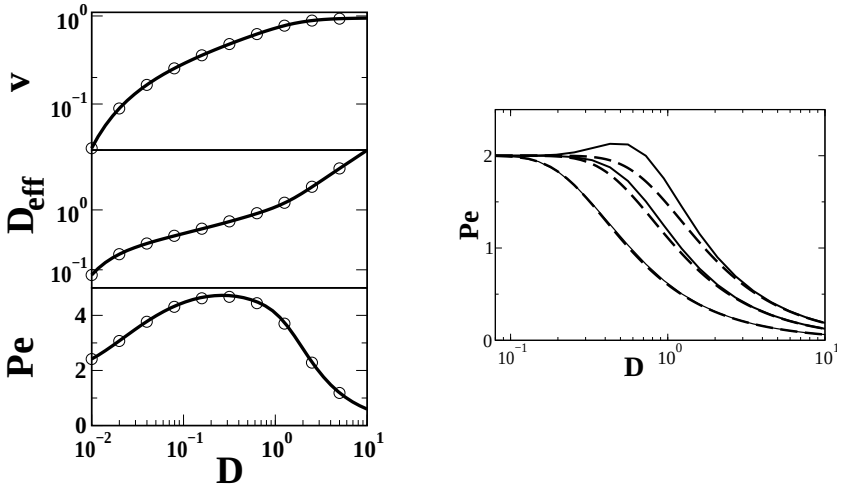


Fig 4. Left: Velocity, diffusion coefficient, and Péclet number according to eqs. (8),(9),(10) versus noise intensity for $F = 0.95$. Circles indicate results from a numerical solution of (2). Right: Péclet number for different tilting forces $F = 0.1, 0.2, 0.3$ (from bottom to top). Theory according to eq. (10) (solid) compared with 'biased-random-walk' approximation eq. (17) (dashed).

At the optimal noise intensity, the motion of the particle is mainly determined by two processes: the noise driven escape from the potential minimum via the right potential barrier followed by a relaxation into the next minimum. The relaxation time depends only weakly on the noise strength and possesses a small variance. The latter fact leads to a certain regularity of the particle motion and accounts for the maximum of the Péclet number.
A weaker maximum of $Pe$ is also observed at smaller tilt. Fig. 4 (r.h.s) shows the Peclet number for $F = 0.1, 0.2, 0.3$ compared to the random walk approximation (17). The latter is sufficient for $F = 0.1$ as well as for small and large noise intensity at arbitrary tilt. It fails, however, to reproduce the nonmonotonous dependence on noise strength that arises numerically for $F > 0.24$.

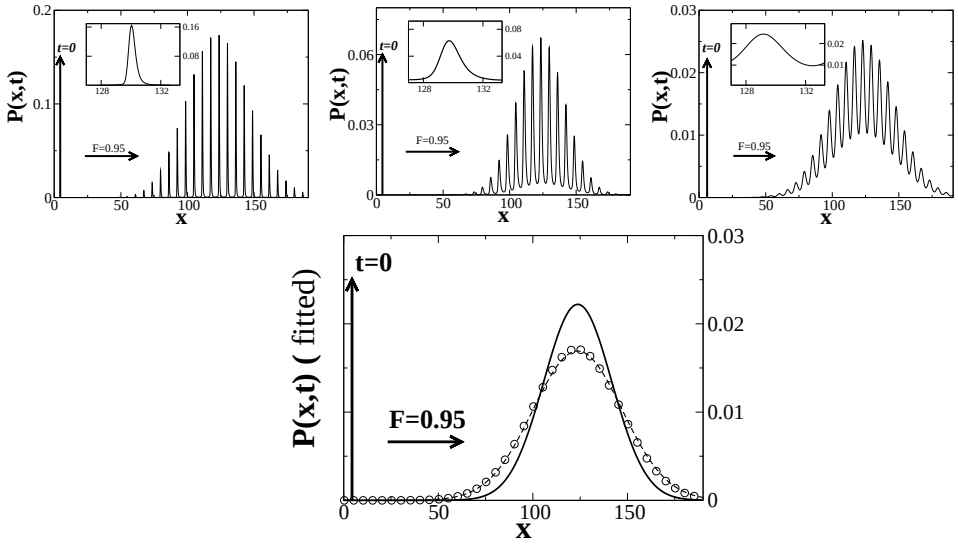


Fig 5. Probability densities versus spatial coordinate for $F = 0.95$ and three different noise levels $D_1 = 0.015$, $D_2 = 0.25$ and $D_3 = 2.05$ at fixed time instances $t \approx 1919, 275$ and 139, respectively. $D_1, D_3$ are chosen such that $Pe(D_1) = Pe(D_3)$ and $D_2$ is the optimal value from Fig. 4. Top: densities obtained by numerical solution of the FPE (2) with $P(x, t = 0) = \delta(x - 4.4)$ (arrow) for $D_1$, $D_2$, $D_3$ (from left to right). The insets show the densities over one period. Bottom: Gaussian fits to these densities, $D_1$ (circles),$D_2$ (solid), $D_3$ (dashed).

The coherent transport for large tilt can be illustrated in the following way. At three different noise intensities $D_1 < D_2 < D_3$ (with $D_2 = D_{max}$ resulting in the maximal Péclet number) an ensemble of particles is started at fixed position $x_0$. The Fokker-Planck equation is integrated until the mean of the respective density reaches a given marker $x_e$. This will, of course, take different times $\Delta t_i$ for the three different noise intensities. For the variances of the densities $\langle \Delta x_i^2 \rangle$ one obtains

$$\langle \Delta x_i^2 \rangle = 2 D_{effi} \Delta t_i = 2 \frac{L v_i \Delta t_i}{Pe_i} = 2 \frac{L(x_e - x_0)}{Pe_i} \ , \quad i = 1, 2, 3. \tag{19}$$

Thus one may conclude that the density at greatest Péclet number will have the smallest variance. This can be verified numerically for the densities depicted in (Fig. 5, top) and is clearly seen when the densities are fitted to Gaussian functions (Fig. 5, bottom). For a given subcritical tilt, the ordered transport of particles from $x_0$ to $x_e$ is thus optimized at finite noise strength.

## 5. Enhanced transport coherence due to a particular potential shape

The optimal transport discussed in the previous section became apparent by a maximum of the Péclet number with respect to the noise intensity. An even stronger coherence of the particle motion emerges for specific potential shapes which generate a long relaxation period and a quick escape at not too small noise intensity noise. Such shape can be realized, for instance, by the potential

$$U(x) = \frac{\Delta}{\varepsilon} e^{\varepsilon(\cos(x)-1)} \tag{20}$$

For large $\varepsilon$ the potential is flat apart from periodically occurring small barriers (cf. Fig. 6, r.h.s., top) the height of which can be scaled by the parameter $\Delta$. If $\Delta$ is negative (cf. Fig. 6, r.h.s., top, black dashed line), the potential exhibits small valleys instead of barriers. For the opposite limit $\varepsilon \to 0$ and fixed $\Delta = 1$ in turn, one recovers the cosine potential.

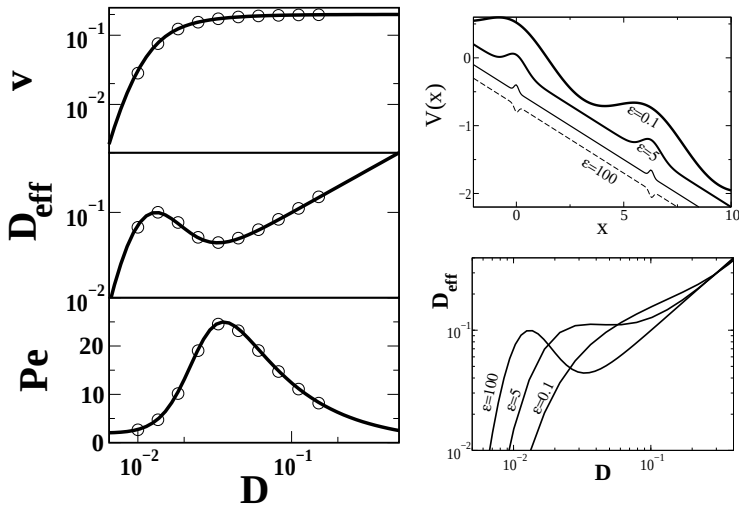


Fig 6. Left: Velocity, diffusion coefficient and Péclet number for the potential eq. (20) according to eqs. (8),(9),(10) versus noise intensity $D$. Circles indicate results from the numerical solution of the FPE (2). Parameters: $\Delta = 10, \varepsilon = 100, F = 0.2$. Right top: The potentials for decreasing values of $\varepsilon = 100, 5, 0.1$ with $\Delta = 10.0, 1.225, 0.282$, respectively. Right bottom: The effective diffusion constant versus noise intensity for the potentials plotted above. The minimum of $D_{eff}$ vanishes at $\varepsilon \approx 5$.

Besides the maximum in the Péclet number we find for large $\varepsilon$ a pronounced minimum in the effective diffusion coefficient at almost the same noise level (see Fig. 6, l.h.s.). This remarkable result (increasing noise decreases diffusion) relies on the

large ratio of relaxation to escape time for the specific potential ($\varepsilon = 100$) at optimal noise intensity. Since the potential tends to a cosine for $\varepsilon \to 0$, we expect the minimum to vanish for decreasing $\varepsilon$. This is shown in Fig. 6 (r.h.s., bottom) for the potentials depicted in Fig. 6 (r.h.s., top). Here, the parameter $\Delta$ was tuned such that the potential barriers to the right and left are the same for all potentials.
Because the potential (20) possesses spatial symmetry we find according to relation (18) the same functions if $\Delta \to -\Delta$, i.e., the same velocity, diffusion coefficient and Péclet number for the potentials drawn as black solid and dashed lines in Fig. 6 (r.h.s., top).
In contrast to the cosine potential, the velocity at the optimal noise intensity is almost saturated ($v \approx F$). Furthermore, the maximal value of $Pe$ exceeds the maximal $Pe$ of a random walk (i.e., the small noise limit with $Pe = 2$) by one order of magnitude. Consequently, a much more pronounced coherence is expected for the same 'experiment' like in the previous section. Indeed, the numerical results in Fig. 7 reveal a larger difference in the dispersions at small, large and optimal noise intensity. In addition, the difference in the times to reach the marker $x_e$ is small for optimal and large noise. Hence, for the special potential the *most coherent diffusive* transport at optimal noise intensity is only slightly slower than the *fastest diffusive* transport at large $D$.

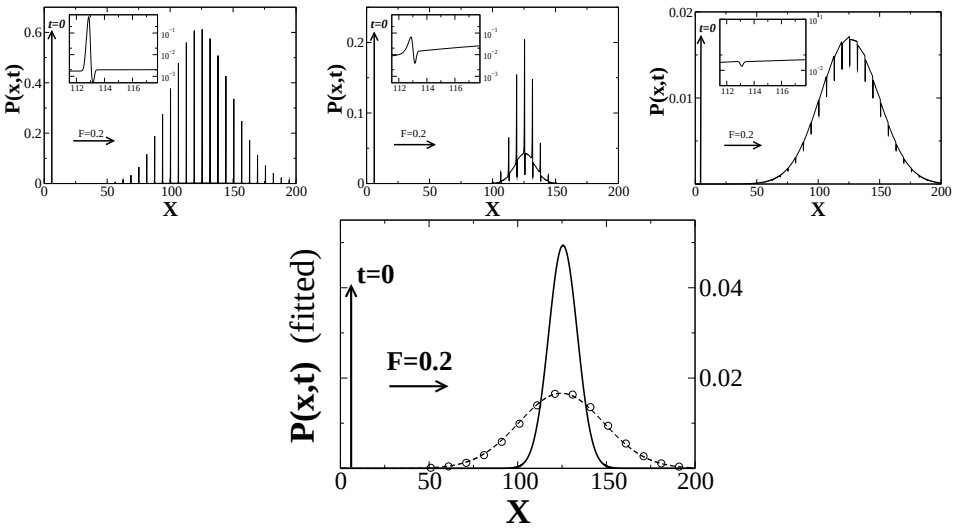


Fig 7. Probability densities versus coordinate for $F = 0.2$ and three different noise levels $D_1 = 0.01$, $D_2 = 0.033$, $D_3 = 0.472$ at fixed time instances $t \approx 4540, 691$ and 625, respectively. $D_1, D_3$ are chosen such that $Pe(D_1) = Pe(D_3)$ and $D_2$ is the optimal value from Fig. 6. Top: densities obtained by numerical solution of the FPE (2) with $P(x, t = 0) = \delta(x - 6.1)$ (arrow), $D_1, D_2, D_3$ (from left to right). The insets show the logarithm of the densities over one period. Bottom: Gaussian fits to these densities, $D_1$ (dashed),$D_2$ (solid),$D_3$ (circles).

The minimum of the diffusion coefficient trivially implies a minimum of the dispersion for the optimal noise intensity when a fixed time instead of a fixed distance is

considered.

## 6. Summary and conclusions

We have derived exact expressions for the diffusion coefficient and the Péclet number of an overdamped Brownian particle in an arbitrary periodic potential with additional tilt. At moderate to strong subcritical bias the Péclet number displays a maximum with respect to the noise intensity indicating a most coherent motion for moderate noise. Especially, for a flat potential with small sharp barriers another effect emerges: the effective diffusion coefficient takes on a local minimum as a function of noise intensity.
The effect of optimal transport is strongly related to the coherence resonance (CR) observed in excitable systems [14] as can be seen in the following. A frequently used measure of this resonance is the coefficient of variation, i.e., the relative standard deviation $R$ of the time interval between subsequent excitations

$$R = \frac{\sqrt{\langle \Delta\tau^2 \rangle}}{\langle \tau \rangle}. \tag{21}$$

As a manifestation of CR, this ratio becomes minimal for a moderate noise intensity, i.e., the excitation sequence is closest to a regular periodic one. In case of the washboard potential it is not obvious how to define a mean time interval since we deal with two different 'excitations': escapes to the left or right side of the segment. If, however, the passage time over one period in direction of the bias [8] is considered we obtain the exact relation (see appendix Appendix B)

$$Pe = \frac{2}{R^2}. \tag{22}$$

It is clearly seen that $Pe$ becomes maximal when $R$ is minimal. A coherence resonance of the above defined passage time hence implies an optimal transport of particles and vice versa.

## Acknowledgements

We acknowledge financial support by DFG: GK 268 (B.L.) and SFB 555 (M.K. and L.S.-G.). M.K. was further supported by KBN Grant No. 2 P03B 160 17 and FNP.

## Appendix A. The discrete process $n_t$

The process $n_t$ depicted in Fig. 3 (r.h.s.) consists of random jumps with random increments $W_i \in \{-1, 1\}$ with probabilities $p_-$ and $p_+$, respectively, at likewise random time instants $t_i$, i.e.,

$$n_t = \sum_{i=1}^{N_t} W_i. \tag{A.1}$$

where $N_t$ denotes the total number of events. Since each realization of an escape event from one segment is independent of all foregoing or subsequent realizations, the escape times $\tau_i = t_i - t_{i-1}$ and increments $W_i$ are independent of all other escape times and increments, respectively. The escape time statistics is given by

the problem illustrated in Fig. 3 (l.h.s.), i.e., by the time dependent FPE (2) with initial condition and absorbing boundary conditions

$$P(x,0) = \delta(x) \qquad P(-L,t) = P(L,t) = 0 \tag{A.2}$$

The absolute values of the outfluxes of probability are related to the conditional escape time densities $\rho_-(\tau)$ and $\rho_+(\tau)$ for left and right jumps, respectively, [13]

$$j_+(t) = p_+\rho_+(\tau) = -D\left.\frac{\partial P(x,t)}{dx}\right|_{x=L} \;,\; j_-(t) = p_-\rho_-(\tau) = D\left.\frac{\partial P(x,t)}{dx}\right|_{x=-L}. \tag{A.3}$$

We now show the surprising property

$$\rho_+(\tau) \equiv \rho_-(\tau) \tag{A.4}$$

that permits the conclusion that there exist no correlations between the escape time $\tau$ and the subsequent jump $W$.
The special Laplace transformation $p(x,\lambda) = \exp[(V(x)-V(0))/2D]\int_0^\infty dt e^{-\lambda t}P(x,t)$ applied to eq. (2) leads to

$$\hat{L}p = Dp''(x,\lambda) - (\frac{(V'(x))^2}{4D} - \frac{V''(x)}{2} + \lambda)p(x,\lambda) = -\delta(x) \tag{A.5}$$

where the prime denotes the derivative with respect to $x$. The (conventional) Laplace transforms of $j_-(t)$ and $j_+(t)$ in terms of $p(x,\lambda)$ are given by

$$J_+(\lambda) = -De^{\frac{FL}{2D}}\left.\frac{\partial p(x,\lambda)}{dx}\right|_{x=L} \;,\; J_-(\lambda) = De^{-\frac{FL}{2D}}\left.\frac{\partial p(x,\lambda)}{dx}\right|_{x=-L} \tag{A.6}$$

It is well known that an equation like (A.5) can be treated by means of homogeneous solutions in $[-L,0]$ and $[0,L]$ which have to be connected according to

$$\lim_{\varepsilon\to 0}(p(\varepsilon,\lambda) - p(-\varepsilon,\lambda)) = 0 \;,\; \lim_{\varepsilon\to 0}(p'(x,\lambda)|_{x=\varepsilon} - p'(x,\lambda)|_{x=-\varepsilon}) = -\frac{1}{D}. \tag{A.7}$$

Provided that $\psi_1(x), \psi_2(x)$ and $\phi_1(x), \phi_2(x)$ (omitting the second argument $\lambda$) are such independent solutions of the homogeneous problem in $[-L,0]$ and $[0,L]$, respectively

$$\hat{L}\psi_{1,2}(x) = 0 \;,\; -L < x < 0 \qquad \hat{L}\phi_{1,2}(x) = 0 \;,\; 0 < x < L \tag{A.8}$$

then we may assume

$$\phi_1(x) = \psi_1(x-L) \;\text{ and }\; \phi_2(x) = \psi_2(x-L) \tag{A.9}$$

because of the periodicity of the force field in (A.5).
The Ansatz

$$p(x,\lambda) = \begin{cases} c_1\psi_1 + c_2\psi_2 \;,\; -L < x < 0 \\ d_1\phi_1 + d_2\phi_2 \;,\; 0 < x < L \end{cases} \tag{A.10}$$

leads by (A.2,(A.7),(A.9) and (A.6) to the following ratio of currents

$$\frac{J_+}{J_-} = \frac{\psi_1'(0)\psi_2(0) - \psi_1(0)\psi_2'(0)}{\psi_1'(-L)\psi_2(-L) - \psi_1(-L)\psi_2'(-L)} e^{\frac{FL}{D}} \tag{A.11}$$

The expression $\psi_1'(x)\psi_2(x) - \psi_1(x)\psi_2'(x)$ which occurs at different argument in the fraction does not depend on the argument $x$. This can be shown by taking the derivative with respect to $x$ and employing (A.8). Hence, we have for arbitrary $\lambda$

$$\frac{J_+(\lambda)}{J_-(\lambda)} = e^{\frac{FL}{D}} = \frac{p_+}{p_-}. \tag{A.12}$$

Obviously, the time dependent currents possess the same ratio and the identity (A.4) is proven.
Since all increments and intervals are independent of each other, the process $n_t$ is a so called *cumulative process with independent increments* whose asymptotic mean and variance are given by [12]

$$\begin{aligned} \langle n_t \rangle &= \langle W \rangle \frac{t}{\mu} \\ \langle \Delta n_t^2 \rangle &= \langle \Delta W^2 \rangle \frac{t}{\mu} + \langle W \rangle^2 \frac{t\sigma^2}{\mu^3}. \end{aligned} \tag{A.13}$$

Here, $\mu$ and $\sigma^2$ are the first two cumulants of the escape time density $\rho(\tau)$. For mean and variance of $W$ one easily verifies

$$\langle W \rangle = p_+ - p_- \ , \ \langle \Delta W^2 \rangle = 4 p_+ p_-. \tag{A.14}$$

Inserting into (A.13) and utilizing eqs. (7), (3), (4), and (6) yield the final results eqs. (8) and (9).

## Appendix B. Equivalence of the result from ref. [8] to formula (9)

In accordance with [8], the velocity and effective diffusion coefficient for $F \geq 0$ are given by

$$v = \frac{L}{\langle T(0 \to L) \rangle} \quad , \quad D_{eff} = \frac{L^2}{2} \frac{\langle \Delta T^2(0 \to L) \rangle}{\langle T(0 \to L) \rangle^3}. \tag{B.15}$$

Here, $\langle T(0 \to L) \rangle$ denotes the mean of the first passage time from 0 to $L$ with absorbing boundary at $-\infty$ and $L$ while $\langle \Delta T^2(0 \to L) \rangle$ is the variance of this time. The formulae (B.15) hold asymptotically for a renewal process corresponding to the discrete mapping depicted in Fig. B.1 (l.h.s.).
Seemingly, the Ansatz in particular at large noise and small bias should fail since the density $p(n)$ is distorted in direction of the bias (obviously, starting an ensemble of particles in the segment with $n = 0$ will not yield any contributions for $n < 0$). Furthermore, it is not obvious which segment number belongs to a certain interval of $x$. However, formula (B.15) emerges to be correct and is equivalent to our results (8) and (9). In order to proof this equivalence we derive and employ a relation between the Laplace transforms of the escape time densities corresponding to finite and infinite segment.

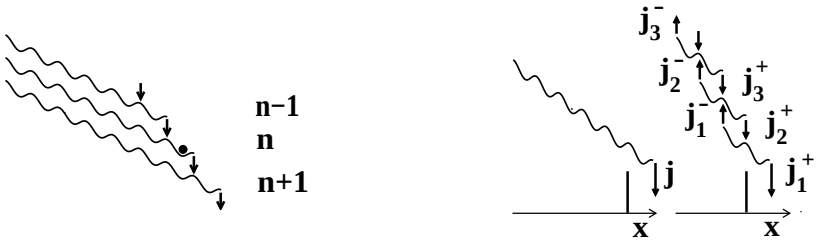


Fig B.1. Left: Renewal process resulting in eqs. (B.15). Right: An ensemble of particles indicated by the thick lines is started at $\tau = 0$, $x = 0$ and absorbed at $x = L$. $j(\tau), j_i^{\pm}(\tau)$ with $i = 1, 2, 3 \cdots$ are the absolute values of the respective probability currents. Note that the numbering of the segments is vice versa to that in Fig. 2 for technical reasons.

The renewal event in the above discretization is the escape out of the single *infinite* segment starting in a distance of one period from the absorbing right boundary (Fig. B.1, middle). It can be expressed by the escape via the corresponding right boundary in an *infinite* number of *finite* segments (Fig. B.1, r.h.s.). The escape time density out of the infinite segment is given by the current $j(\tau)$ which is equal to $j_1^+(\tau)$ (cf. Fig. B.1, middle and r.h.s.) since both discrete descriptions apply to the same physical situation. For the currents $j_n^+$ one obtains

$$\begin{aligned} j_1^+(\tau) &= j(\tau) = p_+\rho(\tau) + p_+ \int_0^\tau d\tau'\; j_2^+(\tau')\rho(\tau - \tau') \\ j_n^+(\tau) &= \int_0^\tau d\tau'\; [p_+ j_{n+1}^+(\tau') + p_- j_{n-1}^+(\tau')]\rho(\tau - \tau')\;,\; n > 1 \end{aligned} \tag{B.16}$$

where we have used the relation $j_n^-(\tau) = j_n^+(\tau)p_-/p_+$ derived in Appendix A. Let $J(\lambda), J_n(\lambda)$ and $\varrho(\lambda)$ be the Laplace transforms of $j(\tau), j_n^+(\tau)$ and $\rho(\tau)$, respectively. Then, eqs. (B.16) lead to a one-sided recurrence relation

$$p_+\varrho J_{n+1} - J_n + p_-\varrho J_{n-1} = 0\;,\quad n \geq 1\;,\quad J_0 \equiv p_+/p_- \tag{B.17}$$

whose solution is given by the periodic continued fraction that can be further simplified [1] to

$$J(\lambda) = J_1(\lambda) = \frac{2p_+\varrho(\lambda)}{1 + \sqrt{1 - 4p_+p_-\varrho(\lambda)^2}}. \tag{B.18}$$

From this relation between the escape time densities the relations between the cumulants $\langle T\rangle, \langle \Delta T^2\rangle$ and $\mu, \sigma^2$ are readily obtained by the first two derivatives of $\ln(J(\lambda))$at $\lambda = 0$ yielding

$$\langle T\rangle = \frac{\mu}{p_+ - p_-}\;,\; \langle \Delta T^2\rangle = \frac{\sigma^2}{p_+ - p_-} + \frac{4p_+p_-\mu}{(p_+ - p_-)^2}. \tag{B.19}$$

For the diffusion constant $D_{eff} = L^2\langle \Delta T^2\rangle/(2\langle T\rangle^3)$ according to eq. (B.15) one recovers our result eq. (9). Hence, the equivalence of both approaches is established.

In addition, from (B.15) we find immediately eq. (22)

$$Pe = 2\frac{\langle T(0 \to L)\rangle^2}{\langle \Delta T^2(0 \to L)\rangle} = \frac{2}{R^2}. \tag{B.20}$$

## References


[1] H. Risken, *The Fokker-Planck Equation*, Springer, Berlin, 1984.

[2] P. Fulde, L. Pietronero, W. R. Schneider, and S. Strässler, Phys. Rev. Lett. **35**, 1776 (1975).

[3] K. Wiesenfeld et. al. Phys. Rev. Lett. **72**, 2125 (1994)

[4] Ch. Kurrer and K. Schulten Phys. Rev. E **51**, 6213 (1995)

[5] R. L. Stratonovich, Radiotekhnika; elctronika **3**, No 4, 497 (1958) [reprint in *Non-Linear Transformations of Stochastic Processes* ed. by P. I. Kuznetsov, R. L. Stratonovich, and V. I. Tikhonov (Pergamon Press, Oxford, 1965)]

[6] R. Festa and E. G. d'Agliano Physica **90 A**, 229 (1978); D. L. Weaver Physica **98 A**, 359 (1979); R. A. Guyer Phys. Rev. B **21**, 4484 (1980); see also [1]

[7] G. Costantini and F. Marchesoni Europhys. Lett. **48** (5), 491 (1999)

[8] P. Reimann, C. Van den Broeck, H. Linke, P. Hänggi, M. Rubi, and A. Perez-Madrid submitted to Phys. Rev. E

[9] L. D. Landau and E. M. Lifschitz *Lehrbuch der Theoretischen Physik* Vol. 6 (Berlin, Akademie-Verlag, 1971)

[10] J. A. Freund and L. Schimansky-Geier, Phys. Rev. E **60**, 1304 (1999)

[11] B. Lindner and L. Schimansky-Geier Phys. Rev. E **60** 7270 (1999).

[12] D. R. Cox *Renewal Theory* (Methuen, London, 1962).

[13] C. W. Gardiner *Handbook of Stochastic Methods* (Springer-Verlag, Berlin, 1985)

[14] A. Pikovsky and J. Kurths Phys. Rev. Lett. **78**, 775 (1997).